



Unsteady 1D Thermally choked Nozzle flow model for low-Mach dual mode scramjet.

J.E. Durand¹ DMPE, ONERA, Université Paris-Saclay F-91123 Palaiseau- France

Abstract

Beyond the flight Mach number 7, the scramjet, with supersonic combustion, shows higher performances than the ramjet, with subsonic combustion, due to the substantial pressure losses, chemical dissociation effects, and high thermomechanical stresses. The dual-mode scramjet would be a solution to hold optimal performances over an extensive range of flight Mach numbers. The use of a divergent nozzle choked through a thermal throat, generated by heat combustion, turns out to be an elegant approach to switch from subsonic to supersonic combustion processes, avoiding mechanical constraints and complex systems. Furthermore, compared with a conventional ramjet, this approach increases the allowable mass flow rate through the engine, increasing the thrust. However, the strong coupling between the thermal throat and the combustion process could lead to complex, unsteady flow behavior, potentially implying the occurrence of critical phenomena such as flame flashback or inlet unstart [1]. The present work aims to develop an unsteady quasi-1D model of a thermally choked nozzle reacting flow. With this model, the analysis of the unsteady behaviors of the aerothermal flow with a thermal throat becomes accessible, improving the quasi-1D dual-mode scramjet combustor simulation. The finite volume method with the WENO5-HLLC scheme is considered. The responses in performance and aerothermodynamics of the flow from changes in the inlet global equivalence ratio are studied.

Keywords: Thermal throat, Dual-mode scramjet, Aerothermal flow, unsteady aerothermodynamics

Nomenclature

A – Section area (m²)

 C_f – Friction coefficient

 D_h – Hydraulic diameter (m)

e - Mass energy (J/kg)

E – Energy (J/m)

h – Height (m)

L - Duct length (m)

m – Mass per unit of distance (kg/m)

M - Mach number

 \dot{m} – Mass flow rate (kg/s)

 N_{esp} – Number of species

P - Pressure (Pa, bar)

T – Temperature (K)

u – Velocity (m/s)

W - Molecular weight (kg/mol)

y – Mass fraction

 β_0 – Oxygen-based vitiation factor

 ϕ – Equivalence ratio

 η – Stoichiometric mixing efficiency

 $\dot{\omega}$ – Species production/deletion rate (kg/m³/s)

Subscripts

b – Fuel to burn

eff – Effective

inlet – Inlet

illiet – Illiet

ch – Chamber

diff – Diffuser

fh - Flame-holder

t - Total

g – Global

O – Oxygen

0 – Origin

tht – Thermal throat

throat – Throat

u - Unburned fuel

p – Combustion products

HiSST-2025-0048
Unsteady 1D Thermally choked nozzle flow model for low-Mach dual mode scramjet.

Page | 1

¹Research Engineer, Energetics Department, jean-etienne.durand@onera.fr

1. Introduction

The dual-mode ramjet configuration using a divergent thermally choked nozzle flow turns out to be an elegant approach to switch from subsonic to supersonic combustion processes, avoiding mechanical constraints and complex systems. Compared with a conventional ramiet combustor, this approach increases the allowable mass flow rate through the engine, increasing the thrust. To assess the performances, the dual-mode ramjet design requires an efficient quasi-one-dimensional combustion chamber model because of the strong flow dependence on the heat release distribution. Numerous quasi-one-dimensional models have been developed, particularly in the last decades [2-5]. O'Brien et al. [6] have given the basis of the finite rate chemistry-based model coupled with the quasi-onedimensional inviscid model of Shapiro [7]. The focus on finite rate chemistry comes from the fact that complex chemistry can also have a direct effect on thrust [2]. In contrast, Birzen & Doolan [8] have proposed a quasi-one-dimensional model with combustion based on mixing-limited rather than chemistry combustion models. According to the authors, this approach is justified when the model is compared with experimental results. Torrez et al. [2] developed a quasi-one-dimensional model, derived from O'Brien ODEs, to investigate the shock and dissociation effects in scramjet engines. The investigators included precombustion shock, fuel mixing, and finite rate chemistry models. The model can solve for both subsonic and supersonic flows [9]. Ispir et al. [10], to develop a robust DMR model for nose-to-tail simulations, use the same formulation. Torrez et al. [3,4,5] then improved the model by considering finite-rate chemistry via the Stationary Laminar Flamelet Model (SLFM). This approach uses a flamelet solution based on an assumed PDF model for each parameter. The probability distribution function (PDF) approach includes the effects of different strain fields, species, and momentum diffusions, and turbulence, as the duct velocity and fuel jet velocity change. The PDF-based chemistry is tabulated [9]. To avoid difficulties in solving the sound speed, the problem is formulated according to velocity instead of the Mach number approach, giving an easier set of equations [11]. This model has been integrated into a scramjet engine model called MASIV [3], developed by the University of Michigan, to predict the thermal throat position and the performance [11]. Zhang et al. [12] have developed a quasi-one-dimensional model by coupling the equations of O'Brien et al. [6] with a regenerative cooling model to study the heat transfer behavior through the cooled scramjet chamber wall. Çakir et al. [13], to assess the performance of intakes for high-speed propulsion systems, use the formulation of Zhang et al. [12] even though the cooling model is not considered. For the TBCC application, Connolly et al. [14] have developed a one-dimensional model in NPSS based on the approach of Smart [15], using a rearranged form of Shapiro's isentropic equations, approximations of the mixing and the combustion heat release of Heiser & Pratt [16], and a simple wall heat flux model. Owing to the structure of NPSS, the model can interface with a cooling system. To rebuild some quantity features of the flow from experimental measurements, Li et al. [17] developed a 1D analysis method based on the classical ODEs for diabatic flow through variable cross sections, rearranged to deduce the Mach number and stagnation temperature from pressure measurements and the geometry. The friction coefficient is, however, set. Seleznev et al. [18] have proposed to compare a quasi-one-dimensional, derived from O'Brien et al. [6] and Birzer et al. [8] approaches, and a two-dimensional model to highlight the elements of the flow field structure not predicted by the quasi-1D model. Tian et al. [19] developed a quasi-one-dimensional method with a new model for precombustion shock trains for simulating the different modes in the dual-mode scramjet flowfield. The release of energy is obtained from a fuel-mixing model or an imposed heat release distribution estimated from experimental results. Frezzotti et al. [20] developed an unsteady quasi-1D model based on the Euler equations, comparing two ways of computing thermodynamics. However, the study is limited to the analysis of combustion instabilities. In the present study, an unsteady 1D model for a thermally choked nozzle flow (UTCNF) is developed to predict unsteady aerothermal flow behavior and performance evolution of a low-Mach dual-mode scramjet engine from operating condition changes during the flight. The model is based on the volume finite method with high-order spatial schemes such as WENO5. The limits of the 1D approach lead to modeling the mixing efficiency to obtain a more realistic feature of the flow found in a low-Mach dual-mode scramjet. The flow and performance responses from slope variation of inlet quantities, such as the equivalence ratio, are analyzed, and the role of the thermal throat is assessed.

2. Methodology

The temporal variations of the thrust depend on the evolution of the aerothermal phenomena in the combustor. However, these processes are highly complex and coupled. An unsteady quasi-onedimensional model of a thermally choked nozzle flow is proposed. To characterize the main phenomena, inlet condition temporal variations are applied, and the flow and performance responses are analyzed. The problem is simplified in one dimension as inlet perturbations have a major impact streamwise. As the combustion process plays a key role in the unsteady aerothermal flow in a dual-mode scramjet combustor, the quasi-1D model considers a finite rate model based on a chemistry kinetic mechanism, in contrast to the model developed by Durand & Olivon [21]. Nevertheless, the presented model is assumed practically inviscid as boundary layers and turbulence effects are not modeled, except the friction. Future studies will consider these aspects to improve the current approach. The temporal evolutions of the thrust, the shock and thermal throat positions, thermodynamic conditions at the thermal and throat, and the exit of the nozzle are analyzed.

2.1. Reference case

The reference case is a typical configuration of a Low-Mach dual-mode scramjet combustor (Fig. 1):

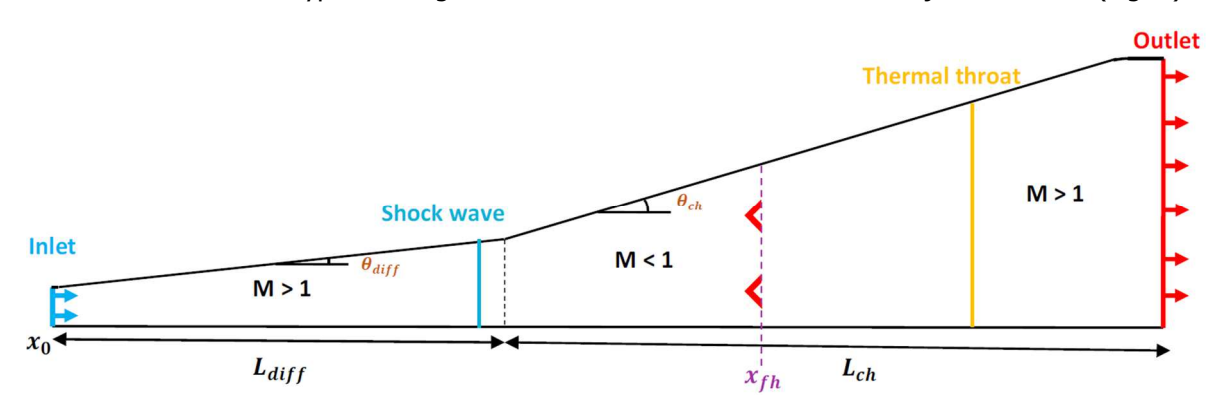


Figure 1. Flow configuration and geometry of the model.

The inlet corresponds to a geometrical throat of a diffuser, introducing the supersonic flow in the combustor. The combustion occurs after the flame-holder position x_{fh} . Table 1 shows the geometrical data used to design the dual-mode scramjet combustor.

Diffuser		Combustor		inlet	flameholder
L _{diff} (m)	θ _{diff} (°)	<i>L_{ch}</i> (m)	θ _{ch} (°)	h _{inlet,throat} (m)	$x_{fh}-x_0$ (m)
1.0	1.5	1.5	3.0	0.01	1.5

Table 1. Design geometry parameters of the reference case

A shock is located in the diffuser, through which the originally supersonic flow becomes subsonic. By releasing the heat of combustion, the flow accelerates, reaching the supersonic regime through a thermal throat. Hence, the inlet supersonic boundary condition requires imposing the values of static temperature, static pressure, velocity, and species composition. At the outlet, no value is imposed as the outflow is supersonic as well. As a first approach, the air/fuel mixing is introduced from the inlet of the flow-field. Nevertheless, to avoid unexpected combustion behavior, a mixing efficiency model is considered.

The imposed values of the sonic incoming flow at the throat of the diffuser are described in Table 2, following the total conditions found at a flight Mach number of 3 and at 11000 m. The fuel is ethylene

HiSST-2024-0048 Page | 3 and is burned with pure Air (no vitiation). The equivalence ratio is chosen according to a relatively poor mixing, as the present study considers the fuel as the unique limiting reagent.

Table 2.	Inlet	condition	of the	reference	case.

P _{inlet} (Pa)	T _{inlet} (K)	M_{inlet}	$\phi_{g,inlet}$
439170	505	1.0	0.78

2.2. Perturbation models

To assess the unsteady behavior of the reacting flow calculated by the quasi-1D model, time dependent parameters, such as the equivalent ratio, static temperature, and the Mach number, are applied to the inlet boundary conditions. Because of the variety of the problem, the present study is limited to the temporal change of the equivalence ratio.

Several kinds of inlet perturbation models exist (forced oscillations, unit impulse, boxcar function, Ricker wavelet, etc.). Nevertheless, the present study is focused on the large time evolution of the equivalence ratio, such as fast monotonic slopes, beyond the assumptions of small perturbations. Hence, Acoustics is not considered.

The reference case shows a configuration with which the residence time is about 6 ms. Hence, three slope intensities are chosen, defined by a transition time from the initial equivalent ratio to the target value (Fig. 2).

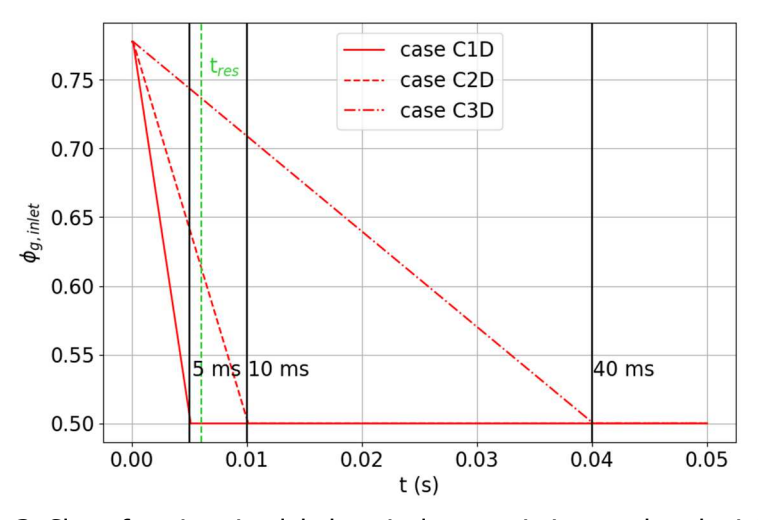


Figure 2. Slope functions in global equivalence ratio imposed at the inlet.

- Case C1D, $dt_{slope} = 5 ms$:
 - The shortest transition time is slightly lower than the residence time, corresponding to the case where the mixing change evolves in the same time as the aerothermal flow;
- Case C2D, $dt_{slope} = 10 ms$:
 - The transition time is higher than the residence time, but the scale is close. Impact of the mixing change is expected, but with lower strength;
- Case C3D, $dt_{slope} = 40 ms$:
 - The longest transition time is higher than six times the residence time, corresponding to the case where the mixing change evolves very slowly.

3. Unsteady 1D thermally choked nozzle model

An unsteady quasi-1D model of a thermally choking nozzle flow is developed to improve the quasi-1D simulation of a dual-mode scramjet.

3.1. Governing equations:

The reacting compressible inviscid flow with friction is assumed in the combustor. The quasi-one-dimensional flow hypothesis is considered, adding a geometrical term in the Euler equations to take into account the section area variations. The chemical creation/production terms are also added to the species transport equations as the combustion is taken into account. These equations are reformulated in a conservative form, particularly for the species transport equations:

$$\frac{\partial W}{\partial t} + \frac{\partial F(W)}{\partial x} = S(W) \tag{1}$$

With:

$$W = \begin{pmatrix} \rho u A \\ \rho e_t A \\ \rho y_1 A \\ \vdots \\ \rho y_{N_{esp}} A \end{pmatrix} = \begin{pmatrix} \dot{m} \\ E_t \\ m_1 \\ \vdots \\ m_{N_{esp}} \end{pmatrix}, F: W \mapsto \begin{pmatrix} \dot{m}u + PA \\ u(E_t + PA) \\ \dot{m}_1 \\ \vdots \\ \dot{m}_{N_{esp}} \end{pmatrix}, S: W \mapsto \begin{pmatrix} P\frac{dA}{dx} - 2C_f \frac{\rho u^2 A}{D_h} \\ 0 \\ \dot{\omega}_1 A \\ \vdots \\ \dot{\omega}_{N_{esp}} A \end{pmatrix}$$

And:
$$m=\sum_{k=1}^{N_{esp}}m_k=\sum_{k=1}^{N_{esp}}\rho y_k A=\rho A \ \& \ u=\frac{\dot{m}}{m}$$

The Euler variables are transformed to take into account the section area, invariant in time (fixed & rigid geometry). Hence, a new variable vector is built. The total energy includes not only the kinetic energy but also the sensible energy and the formation enthalpy. Hence, the expression of the reaction term in the energy equation is not required. The equation system is closed with the ideal gas law. Nevertheless, the heat capacity is determined from the NASA polynomial parametrizations [22].

The hydraulic diameter is obtained as twice the height of the cross section, considering the wetted surface located only on the upper and the lower surfaces, as plane geometry is assumed with a z-axis invariance. The friction coefficient is determined by using the correlation of De Chant *et al.* [23], developed for compressible flow, assuming smooth walls (k+=0). Nevertheless, the related dissipation term of the energy equation is neglected.

As in the study of O'Brien *et al.* [5], a finite-rate chemistry model is used, based on kinetic mechanisms. Even though a complex mechanism could be chosen, and because the object of the study is not the impact of chemistry, a one-step oxidation mechanism of ethylene is considered (Westbrook & Dryer) in the present work.

3.2. Mixing efficiency model:

In the present study, to improve the representation of aerothermal 1D flow modeled with a chemical kinetic mechanism and Euler equation system, a mixing model efficiency is introduced. In the chemical sources, instead of using the full value of the fuel mass fraction given by the flow, only the effective fuel mass fraction is considered. The stoichiometric mixing efficiency definition is used:

$$\eta = \frac{\int_{A} y_{O} \min(1, \phi) dm - \dot{m}_{O, p}}{\int_{A} y_{O, g} \min(1, \phi_{g}) dm - \dot{m}_{O, p}}$$
(2)

This efficiency (Eq. 2) is defined as the ratio of oxygen mass flow rate potentially to be burned in heterogeneous mixing over the oxygen mass flow rate in homogeneous mixing. In multidimensional flows, the inhomogeneity of the flow creates mixed regions ready to burn and other regions where the

HiSST-2024-0048 Page | 5

mixing is either too poor or too rich, leading to a stoichiometric mixing efficiency less than unity. In the present case, the 1D hypothesis leads to develop a simple mixing model, considering two flows, of which one is the unburned pure fuel and the other the mixture at equivalence ratio ϕ_{eff} . Hence, the efficiency can be written as:

$$\eta = \frac{\int_{A_b} y_O \min(1,\phi) dm + \int_{A_u} y_O \min(1,\phi) dm - \dot{m}_{O,p}}{\int_A y_{O,g} \min(1,\phi_g) dm - \dot{m}_{O,p}} = \frac{\dot{m}_O \min(1,\phi_{eff}) - \dot{m}_{O,p}}{\dot{m}_O \min(1,\phi_g) - \dot{m}_{O,p}}$$
(3)

 $\dot{m}_{O,p}$ is the oxygen mass flow rate of combustion products from the upstream. The effective equivalence ratio ϕ_{eff} can be expressed as a function of the mixing efficiency and the global equivalence ratio:

$$if \ \phi_{eff} < 1, \ \phi_{eff}(\mathbf{x}) = \beta_0 + \eta \left(\min(1, \phi_g) - \beta_0 \right) \tag{4}$$

With $\beta_0 = \frac{m_{0,p}}{m_0}$. In the present study, only poor mixings are considered. Nevertheless, the rich mixing case will be treated in further studies. Using the equivalence ratio definition, Eq. 4 and Eq. 5, the effective fuel mass fraction turns out to be proportional to the stoichiometric mixing efficiency:

$$y_{fuel,eff} \propto \frac{\eta y_0 \phi_g}{\phi_g} \left(\min(1, \phi_g) - \beta_O \right)$$
 (5)

The efficiency variations are empirically modeled.

4. Numerical setup

4.1. Numerical methods

The numerical discretization method for solving Eq. 1 follows the finite volume approach. The flux calculation is based on the approximate Riemann solver HLLC [24]. The flux reconstruction is realized with a fifth-order weighted essentially non-oscillatory (WENO) method [25].

The time discretization follows the approach of Strang [26], consisting of decoupling each term of the conservative equations (advection, diffusion, and source terms). The method performs three integration steps with a symmetrical structure. Firstly, the ODE with the advection terms is explicitly integrated. In the second step, the ODE with the source terms is integrated according to the semi-implicit method ODEPIM [27]. Then, in the last step, explicit integration of the advection term is performed again. For the time explicit discretization, an equivalent form of the 3rd order TVD (Time-variation-diminishing) Runge-Kutta method is employed [28]. The global time step is obtained to hold a CFL number less than unity.

4.2. Mesh

The mesh is designed with nodes regularly spaced. The computations are performed for a mesh with 6000 cells.

5. Discussion & results

The steady computation is performed to obtain the reference fields of Mach number, temperature, pressure, and species mass fractions (Fig. 3 & Fig. 4). As expected, a subsonic region is formed between the shock wave ($x \sim 1$ m) and the thermal throat ($x \sim 1.66$ m) due to the combustion process.

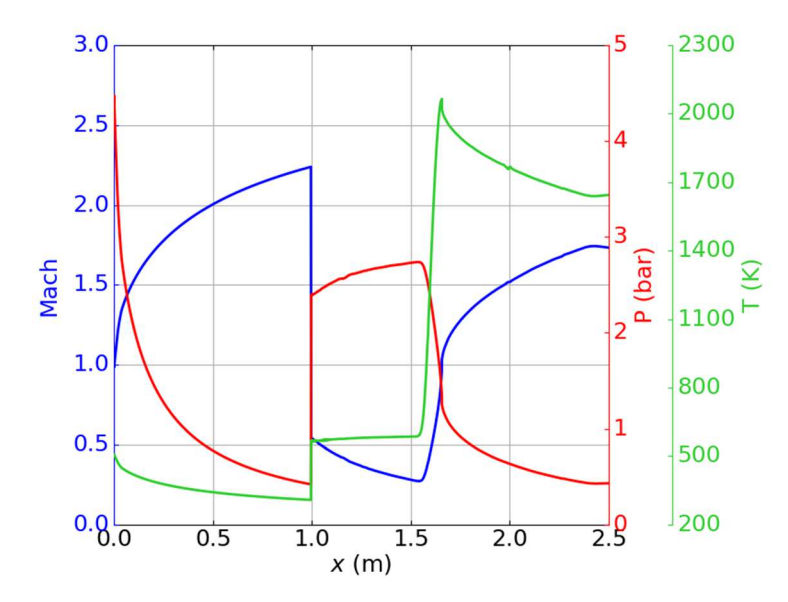


Figure 3. Mach number, temperature and pressure variations along the combustor.

The combustion starts slowly from the position of the flame-holder, until increasing sharply (Fig. 4). This smooth transition is due to the mixing efficiency model. According to the species mass fraction variations, the combustion process is short, with a progressive temperature decrease since x = 1.66 m. In the subsonic region, the pressure reaches a stage around 2.4-2.75 bar.

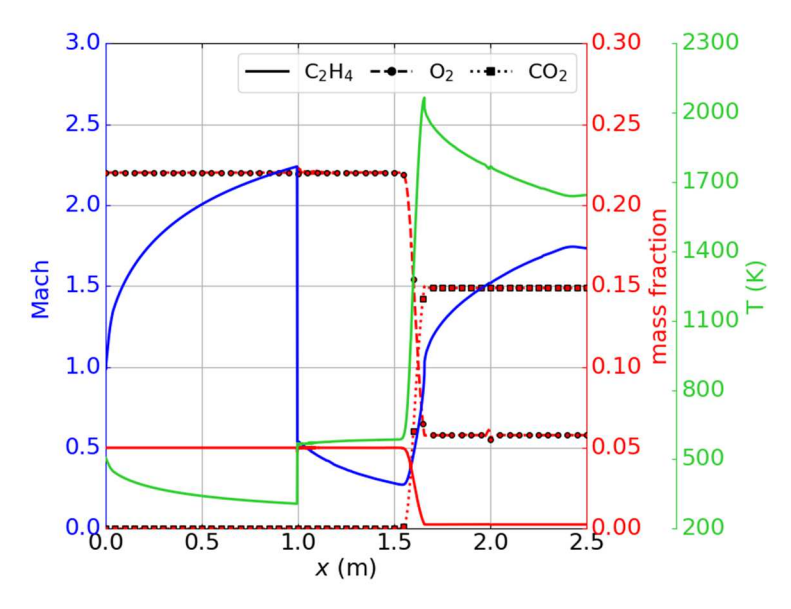


Figure 4. Mach number, temperature and main species variations along the combustor.

The shock wave is located almost on the boundary between the diffuser and the chamber ducts, as expected according to the chosen design of the aperture angle of the diffuser and the chamber.

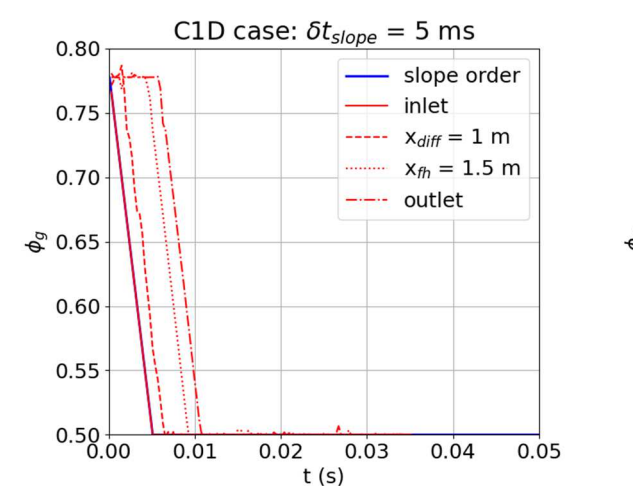
5.1. Effects of the slope intensity of equivalent ratio on the thrust

When applying the slope functions at the inlet of the reference cases, a delay of the responses of the flow is recorded (Fig. 5 & Fig. 6). The time difference between the inlet of the chamber and the thermal throat position is particularly large compared with the distance through which the global equivalence ratio change propagates. The main reason is that the flow is subsonic in this region, compared with the two other supersonic regions. On another hand, the shortest and the longest transition time cases show

HiSST-2024-0048

Page | 7

the same pattern, preserving the temporal trend of the slope. The local equivalence ratio temporal evolution is therefore invariant in slope value.



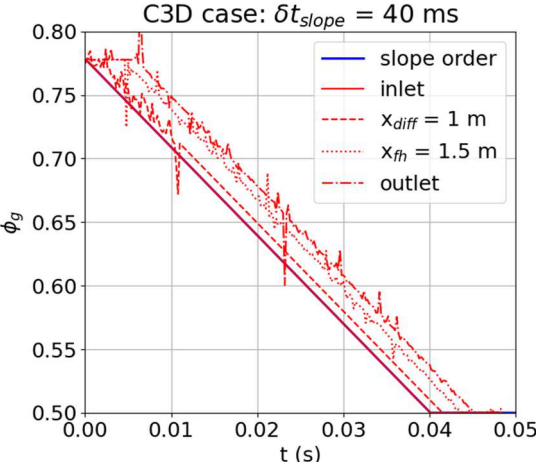


Figure 5. Global equivalence ratio evolution during the slope process through the combustor, x = 5 ms.

Figure 6. Global equivalence ratio evolution during the slope process through the combustor, x = 40 ms.

The thrust decrease due to the equivalence ratio decrease evolves more smoothly, following a curvy trend instead of a linear one (Fig. 7). This pattern reflects the time evolution of the outlet pressure, as the thrust is an integrated form of the pressure distribution through the nozzle, instead of the outlet temperature, with a stricter linear decrease. All of these trends begin decreasing after a delay close to the residence time (\sim 6 ms), as these values are measured at the outlet of the combustor.

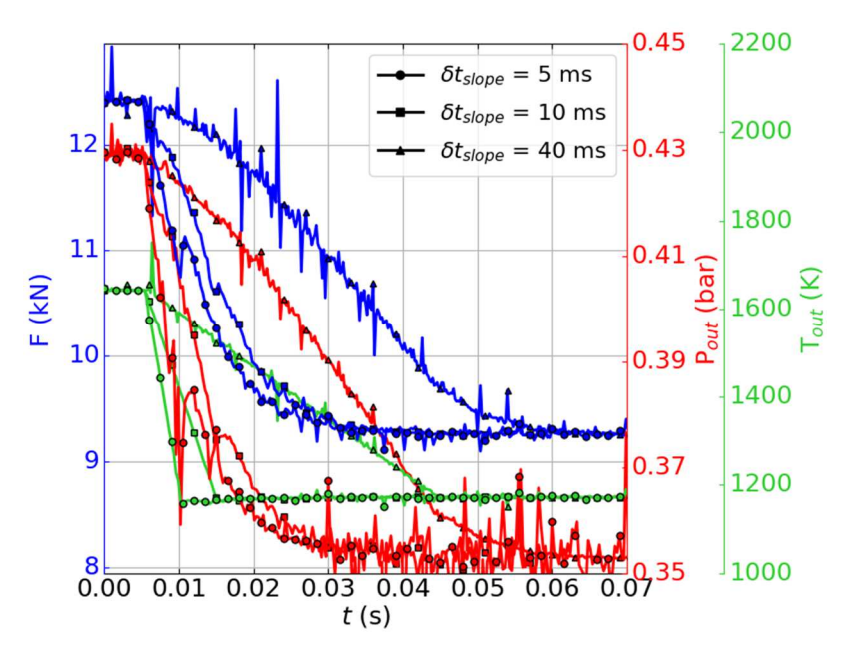


Figure 7. Thrust and outlet conditions evolution during the slope process for each studied case.

Furthermore, the transition time of the thrust and static pressure reaches a stabilized value is significantly larger than the transition time of the equivalence ratio slope decrease (Table 3). Nevertheless, when the transition time is close to the residence time (C1D & C2D cases), the transition time of the thrust & static pressure seems very similar even though the inlet equivalence ratio slopes display twice longer transition time for C1D compared with C2D. However, for the case C3D, the transition time for the thrust and pressure is much larger than the other cases, even though the

difference in the transition time of the inlet equivalence ratio slope is much smaller than the other cases.

Tableau 3. Transition time difference between the thrust temporal evolution and the inlet equivalence ratio decrease.

Slope cases	C1D	C2D	C3D
$t_{transition, \phi_g}$ (ms)	5	10	40
$t_{transition, thrust}$ (ms)	~ 24	~ 24	~ 54
$\frac{\Delta t_{transition}}{t_{transition, \phi_g}} (\%)$	~ 380	~140	~ 35

Hence, the order of magnitude of the transition time of the inlet equivalence ratio slopes significantly changes the temporal response of the compressible flow.

5.2. Effects of the slope of equivalence ratio on the flow structure and the thermal throat

The decrease in equivalence ratio reduces the combustion intensity, indicated by the decrease of the maximum temperature value in Fig. 8. Due to the combustion intensity decrease, the subsonic region size becomes smaller. However, the trends differ between the shock wave and the thermal throat positions. The thermal throat follows the trends of the equivalence ratio with an almost linear displacement upstream, whereas the shock wave position displays convex curves for the transition times of 5 ms and 10 ms. For 40 ms, the curve tends to be concave.

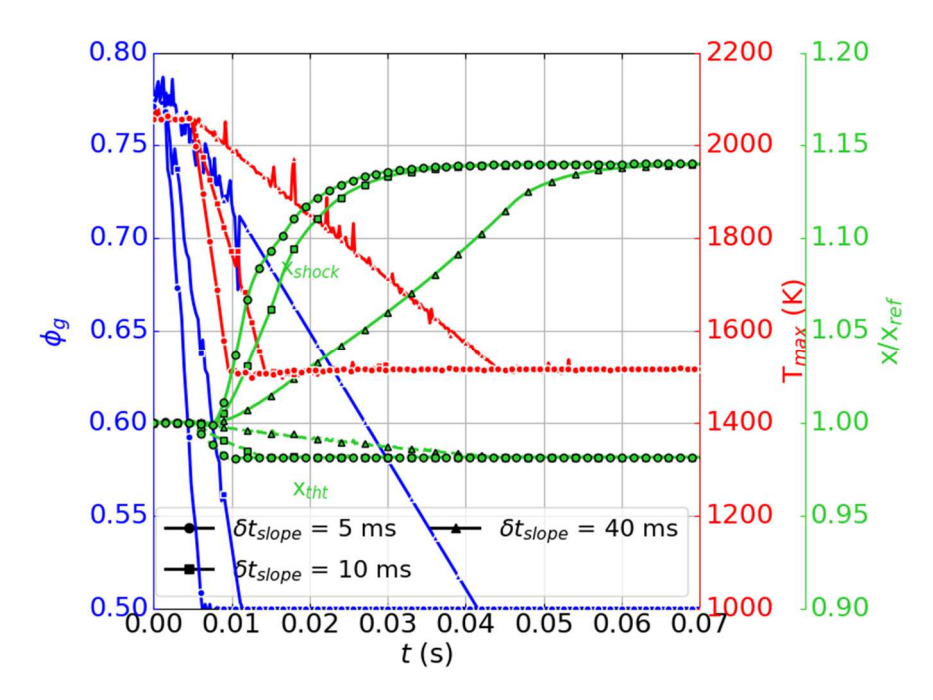


Figure 8. Impact of the equivalence ratio evolution on the aerothermal condition in the combustor

The shock wave behavior reflects the trends observed for the outlet and critical pressures (Fig. 9). The unsteady behavior of the thrust is therefore predominantly driven by the compressible flow structure rather than the temporal trends of the combustion process.

On the other hand, the thermal throat position, critical and maximum temperatures are strongly related to the slope of the equivalence ratio, showing a threshold when the set-point is reached. Hence, the unsteady behavior of the thermal throat and the combustion process is mainly ruled by the time evolution of the global equivalence ratio.

HiSST-2024-0048 Page | 9

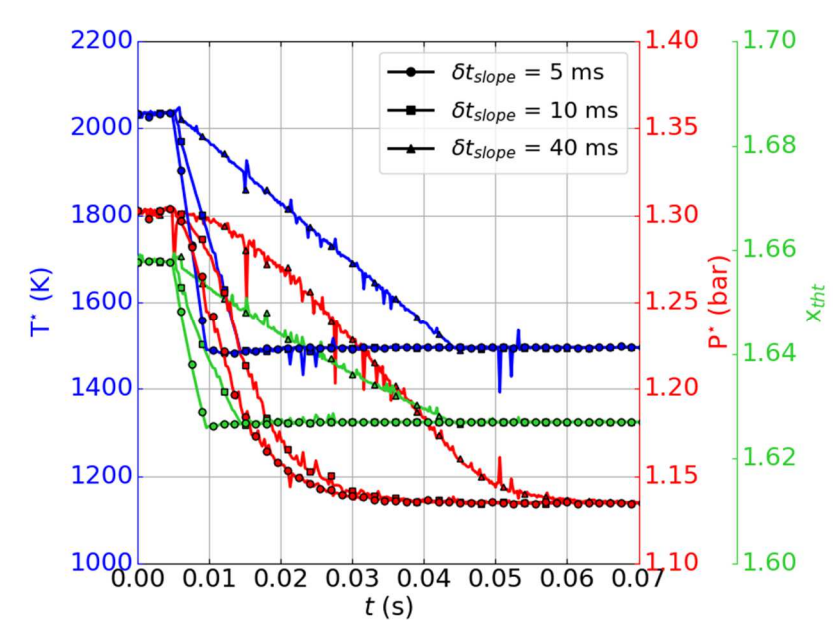


Figure 9. Critical condition evolution during the slope process.

6. Conclusion & perspectives

A new unsteady quasi-1D model of a thermally-choked nozzle is developed, based on the finite volume approach with the WENO5-HLLC scheme. The present study considers the unsteady performance and aerothermal flow response to the temporal evolution of the global equivalence ratio. The slope function is chosen as a non-periodic and large temporal perturbation, imposed at the inlet of the dual-mode scramjet combustor configuration. Even though the transition times are quite short, the static temperature and the thermal throat position follow strictly the trend of the global equivalence ratio slope, displaying a strong unsteady link between the thermal throat and the equivalence ratio. The thrust temporal behavior is related to the evolution of static pressure in the combustor and to the displacement of the shock wave. The time response of those quantities is much larger than that of the ones related to the thermochemistry. The unsteady behavior of the propulsive performance is therefore driven mainly by the response of the compressible flow.

The present study will be extended to include other inlet parameters and slope functions to confirm and validate the presented observation. On the other hand, some physical models, such as the mixing efficiency model, have to be validated in unsteady conditions. Oscillations of the solution appear during the slope process, which must be investigated. In future development, new features such as improved mixing efficiency, turbulence effects, boundary layer, recirculation zone, and shock train models will be considered and added.

References

- 1. Laurence, S. J., Karl, S., Schramm, J. M., & Hannemann, K. (2013). Transient fluid-combustion phenomena in a model scramjet. Journal of Fluid Mechanics, 722, 85-120.
- 2. Torrez, S., Driscoll, J., Bolender, M., Oppenheimer, M., & Doman, D. (2008). Effects of improved propulsion modelling on the flight dynamics of hypersonic vehicles. In *AIAA Atmospheric Flight Mechanics Conference and Exhibit* (p. 6386).
- 3. Torrez, S. M., Driscoll, J., Dalle, D., and Daniel Micka. "Scramjet Engine Model MASIV: Role of Mixing, Chemistry and Wave Interaction," AIAA 2009-4939. *45th AIAA/ASME/SAE/ASEE Joint Propulsion Conference & Exhibit*. August 2009.

- 4. Torrez, S. M., Driscoll, J., Dalle, D., Michael Bolender and David Doman. "Hypersonic Vehicle Thrust Sensitivity to Angle of Attack and Mach Number," AIAA 2009-6152. *AIAA Atmospheric Flight Mechanics Conference*. August 2009.
- 5. Torrez, S. M., Driscoll, J., Dalle, D., and Fotia, M. "Preliminary Design Methodology for Hypersonic Engine Flowpaths," AIAA 2009-7289. *16th AIAA/DLR/DGLR International Space Planes and Hypersonic Systems and Technologies Conference*. October 2009.
- 6. O'Brien, T. F., Starkey, R. P., and Lewis, Mark J., Quasi-One-Dimensional High-Speed Engine Model with Finite-Rate Chemistry, Journal of Propulsion and Power 2001 17:6, 1366-1374.
- 7. Shapiro, A., The Dynamics and Thermodynamics of Compressible Fluid Flow, Vol. 1, Ronald Press, New York, pp. 226-227
- 8. Birzer, C. H., & Doolan, C. J. (2009). Quasi-one-dimensional model of hydrogen-fueled scramjet combustors. *Journal of propulsion and power, 25*(6), 1220-1225.
- 9. Torrez, S. M., Driscoll, J. F., Ihme, M., & Fotia, M. L. (2011). Reduced-order modeling of turbulent reacting flows with application to ramjets and scramjets. *Journal of propulsion and power*, 27(2), 371-382.
- 10. Ispir, A. C., and Saracoglu, B.H. "Development of a 1D dual mode scramjet model for a hypersonic civil aircraft," AIAA 2019-3842. *AIAA Propulsion and Energy 2019 Forum.* August 2019.
- 11. Torrez, S. M., Dalle, D. J., & Driscoll, J. F. (2013). New method for computing performance of choked reacting flows and ram-to-scram transition. *Journal of Propulsion and Power, 29*(2), 433-445.
- 12. Zhang, D., Feng, Y., Zhang, S., Qin, J., Cheng, K., Bao, W., & Yu, D. (2016). Quasi-one-dimensional model of scramjet combustor coupled with regenerative cooling. *Journal of Propulsion and Power, 32*(3), 687-697.
- 13. Cakir, B. O., Ispir, A. C., & Saracoglu, B. H. (2022). Reduced order design and investigation of intakes for high speed propulsion systems. *Acta Astronautica*, *199*, 259-276.
- 14. Connolly, B. J., Krouse, C. R., & Musgrove, G. O. (2021). Implementing a dual-mode scramjet combustor model in NPSS. In *AIAA Propulsion and Energy 2021 Forum* (p. 3538).
- 15. Smart, M. (2007). Scramjets. The Aeronautical Journal, 111(1124), 605-619
- 16. Heiser, W. H., & Pratt, D. T. (1994). Hypersonic airbreathing propulsion. Aiaa.
- 17. Li, J., Jin, R., Jiao, G., & Song, W. (2018). Analysis on mode transition in a dual-mode scramjet combustor. *Combustion Science and Technology*, *190*(1), 82-96.
- 18. Seleznev, R. K. (2017, February). Comparison of two-dimensional and quasi-one-dimensional scramjet models by the example of VAG experiment. In *Journal of Physics: Conference Series* (Vol. 815, No. 1, p. 012007). IOP Publishing.
- 19. Tian, L., Chen, L., Chen, Q., Li, F., & Chang, X. (2014). Quasi-one-dimensional multimodes analysis for dual-mode scramjet. *Journal of Propulsion and Power*, *30*(6), 1559-1567.
- 20. Frezzotti, M. L., D'Alessandro, S., Favini, B., & Nasuti, F. (2017). Numerical issues in modeling combustion instability by quasi-1D Euler equations. *International Journal of Spray and Combustion Dynamics*, *9*(4), 349-366.
- 21. Durand, J.E. & Olivon, F. (2024). Thermally choked nozzle flow 1D model for low-Mach dual mode ramjet performance assessment. 3rd International Conference on High-Speed Vehicle Science & Technology, 0130.
- 22. McBride, B. J., Zehe, M. J., & Gordon, S. (2002). *NASA Glenn Coefficients for Calculating Thermodynamic Properties of Individual Species* (No. NASA/TP-2002-211556).
- 23. Dechant, L. J. & Tattar, M. J. (1994). *Analytical skin friction and heat transfer formula for compressible internal flows* (No. NASA-CR-191185).

HiSST-2024-0048 Page | 11

- 24. Toro, E. F. "The HLL and HLLC Riemann solvers." *Riemann Solvers and Numerical Methods for Fluid Dynamics: A Practical Introduction*. Berlin, Heidelberg: Springer Berlin Heidelberg, 2009. 315-344.
- 25. Jiang, G. S. & Shu, C. W. (1996). Efficient implementation of weighted ENO schemes. *Journal of computational physics*, *126* (1), 202-228.
- 26. Strang, G. On the construction and comparison of difference schemes. SIAM J. Numer. Anal., 5(3):506–517, 1968.
- 27. Liang, L., Kong, S. C., Jung, C. and Reitz, R.D. Development of semi-implicit solver for detailed chemistry in internal combustion engines simulation. J. Eng. Gas Turbine. Power, 129:271–278,2007.
- 28. Shu, C. W. & Osher, S. Efficient implementation of essentially non-oscillatory shock-capturing schemes, J. Comput. Phys., 77 (1988), pp. 439–471.

HiSST-2025-0048 Page | 12 J.-E. Durand Copyright © 2025 by author(s)